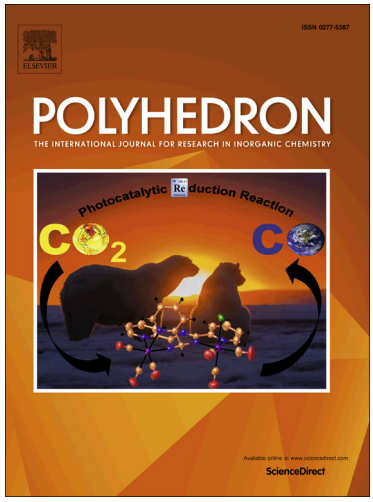

Oxidative bromination of monoterpene (thymol) using dioxidomolybdenum (VI) complexes of hydrazones of 8-formyl-7-hydroxy-4-methylcoumarin

Mannar R. Maurya, Sarita Dhaka, Fernando Avecilla

PII: S0277-5387(15)00242-9
DOI: http://dx.doi.org/10.1016/j.poly.2015.05.001
Reference: POLY 11299

To appear in: *Polyhedron*

Received Date: 29 March 2015
Accepted Date: 1 May 2015

Please cite this article as: M.R. Maurya, S. Dhaka, F. Avecilla, Oxidative bromination of monoterpene (thymol) using dioxidomolybdenum (VI) complexes of hydrazones of 8-formyl-7-hydroxy-4-methylcoumarin, *Polyhedron* (2015), doi: http://dx.doi.org/10.1016/j.poly.2015.05.001

Oxidative bromination of monoterpene (thymol) using dioxidomolybdenum (VI) complexes of hydrazones of 8-formyl-7-hydroxy-4-methylcoumarin

Mannar R. Maurya [a,*], Sarita Dhaka [a], Fernando Avecilla [b]

[a] *Department of Chemistry, Indian Institute of Technology Roorkee, Roorkee 247 667, India.*

[b] *Departamento de Química Fundamental, Universidade da Coruña, Campus de A Zapateira, 15071 A Coruña, Spain*

Keywords: Tridentate ONO Donor Schiff base ligands; Molybdenum(VI) complexes; NMR spectroscopy; Oxidative bromination of thymol.

* Corresponding author. Tel.: +91 1332 285327; fax: +91 1332 273560.

E-mail address: rkmanfcy@iitr.ac.in (M.R. Maurya).

ABSTRACT

Condensation of equimolar amount of 8-formyl-7-hydroxy-4-methylcoumarin (fhmc) and hydrazides [benzoylhydrazide (bhz), isonicotinoylhydrazide (inh), nicotinoylhydrazide (nah) and furoylhydrazide (fah)] in methanol results in the formation of potential ONO tridentate ligands H_2fhmc-bhz (**I**), H_2fhmc-inh (**II**), H_2fhmc-nah (**III**), and H_2fhmc-fah (**IV**), respectively. Reaction of these ligands with $[Mo^{VI}O_2(acac)_2]$ in refluxing methanol gives dioxidomolybdenum(VI) complexes, $[Mo^{VI}O_2$(fhmc-bhz)(MeOH)] (**1**), $[Mo^{VI}O_2$(fhmc-inh)(MeOH)] (**2**) $[Mo^{VI}O_2$(fhmc-nah)(MeOH)] (**3**) and $[Mo^{VI}O_2$(fhmc-fah)(MeOH)] (**4**), respectively. The structures of the obtained ligand and their respective metal complexes were elucidated by elemental analyses, spectroscopic techniques (IR, electronic, ^{1}H and ^{13}C NMR) and thermogravmetric analyses. Single crystal X-ray analysis of complex **1** confirms the chelation of the ligand to the metal ion through two oxygen and a nitrogen atoms. These metal complexes have been tested against oxidative bromination of monoterpene (thymol) to yield 2-bromothymol, 4-bromothymol and 2,4-dibromothymol using H_2O_2 as an oxidant therefore they act as functional models of vanadium dependent haloperoxidases. The effects of various factors, such as amounts of catalyst, oxidant, KBr, $HClO_4$ and different solvents have been considered to optimize the reaction conditions for the maximum brominated products.

1. Introduction

Terpenes are extremely miscellaneous division of natural products from which numerous commercial compounds are derived. Their potential therapeutic properties in pharmaceutical (like anticancer, anti-microbial and anti-inflammatory), uses in sanitary, cosmetic, agricultural and food industries, and making flavor and fragrance related compounds further show their importance [1]. Particularly monoterpenes represent a cheap and most abundant source of chiral substances that can be transformed into valuable bioactive compounds [2]. The most common thyme oil (thymus vulgaris) contains 20–54% thymol [3] which is an antiseptic and is the main active constituent of various mouth washes and has also been found to be effective against various fungi.

Coumarins are oxygen containing heterocyclic compounds, which show their significance in the territory of natural products and synthetic organic chemistry [4]. Coumarin and its

derivatives have been a subject of several investigations due to their miscellaneous biological activities [5,6], interesting photophysical, photochemical and metal binding properties. It has been found that the coordination of coumarin moiety to metal preserves or even boosts its biological activity [6,7]. They can also provoke modification in cell growth, development of intracellular communication mechanisms. Many coumarins are selective coronary vasodilators [8] and possess radioactive properties [9].

The hydrazones are relatively cheap and environmentally endurable ligands, which can be synthesize through simple synthetic procedures [10-12]. Hydrazone moieties are the most important pharmacophoric cores of several anti-inflammatory, antinociceptive, and antiplatelet drugs [13]. Their *cis*-$[Mo^{VI}O_2]^{2+}$ complexes have shown interesting antibacterial [10] and catalytic activities [11]. Catalytic activities of *cis*-$[Mo^{VI}O_2]^{2+}$ complexes of other ONO donor ligands have also been well documented in the literature [12,14-16].

The aim of the present work is to synthesize and characterize new *cis*-$[Mo^{VI}O_2]^{2+}$ complexes with newly synthesized hydrazones of 8-formyl-7-hydroxy-4-methylcoumarin (Scheme 1) and use them as catalyst precursor towards the oxidative bromination of monoterpene (thymol). Brominated compounds are the most plentiful organohalides in environment. This category of molecules get usages in various fields such as agrochemicals and pharmaceuticals, Furthermore, brominated derivatives are regarded as significant synthetic intermediates for numerous selective and efficient transformations [17, 18]. Only few examples of thymol bromination reaction are reported in the literature [19-22].

<<Scheme 1>>

2. Experimental Section

2.1. Materials

Analytical reagent grade ammonium molybdate, ethyl benzoate, hydrazine hydrate, isonicotinoylhydrazide (Loba Chemie, Mumbai, India), nicotinoylhydrazide (Acros organics, New Jersey, USA), furoylhydrazide, (Aldrich Chemicals Co., U.S.A.), acetylacetone, thymol (Himedia), 30% aqueous H_2O_2, (Rankem, New Delhi, India), were used as obtained. $[Mo^{VI}O_2(acac)_2]$ [23] and 8-formyl-7-hydroxy-4-methylcoumarin [24] were prepared according

to methods reported in the literature. Benzoylhydrazide was prepared by the reaction of a twofold excess of hydrazine hydrate with ethyl benzoate in ethanol.

2.2. Instrumentation and characterization Procedures

Elemental analysis of the compounds was carried out on an Elementar model Vario-El-III. Thermogravimetric analysis was carried out under an oxygen atmosphere using a TG Stanton Redcroft STA 780 instrument. IR spectra were recorded as KBr pellets on a Nicolet NEXUS Aligent 1100 series FT-IR spectrometer. Electronic spectra of ligand and complexes were recorded in DMSO using Shimadzu 2450 UV-VIS spectrophotometer. ^{1}H and ^{13}C NMR spectra of complexes were recorded on a Bruker Avance 500 MHz spectrometer with the common parameter settings in DMSO-d_6. The δ values are quoted relative to TMS as internal standard. A Shimadzu 2010 plus gas-chromatograph fitted with a Rtx-1 capillary column (30 m × 0.25 mm × 0.25 μm) and a FID detector was used to analyze the catalytic reaction products. The identity of the products was confirmed using a GC-MS model Perkin-Elmer, Clarus 500 by comparing the fragments of each product with the library available. The percent conversion of substrate and selectivity of products were calculated from GC data using the formulae presented elsewhere. [25]

2.3. Preparations

*2.3.1. Preparations of H_2fhmc-bhz (**I**), H_2fhmc-inh (**II**) H_2fhmc-nah (**III**) and H_2fhmc-fah (**IV**)*

All ligands were prepared using a general procedure. A representative preparation is presented here. A solution of 8-formyl-7-hydroxy-4-methylcoumarin (2.04 g, 10 mmol) in methanol (20 ml) was mixed to a filtered solution of benzoylhydrazide (1.36 g, 10 mmol) in methanol (20 ml) with stirring and the obtained reaction mixture was refluxed on a water bath for 4 h. The resulted solid was filtered after cooling, washed with methanol and dried over silica gel under vacuum.

H_2fhmc-bhz (**I**): Yield: 2.50 g (77.6%). *Anal.* Calc. for $C_{18}H_{14}N_2O_4$ (322.30): C, 67.07; H, 4.38; N, 8.69 %. Found: C, 67.19; H, 4.32; N, 8.72%.

H_2fhmc-inh (**II**): Yield: 2.45 g (75.8%). *Anal.* Calc. for $C_{17}H_{13}N_3O_4$ (323.30): C, 63.16; H, 4.05; N, 13.00 %. Found: C, 63.08; H, 4.15; N, 13.12%.

H_2fhmc-nah (**III**): Yield: 2.47 g (76.4%). *Anal*. Calc. for $C_{17}H_{13}N_3O_4$ (323.30): C, 63.16; H, 4.05; N, 13.00 %. Found: C, 63.10; H, 4.11; N, 13.09%.

H_2fhmc-fah (**IV**): Yield: 2.39 g (76.6%). *Anal*. Calc. for $C_{16}H_{12}N_2O_5$ (312.28): C, 61.54; H, 3.87; N, 8.97 %. Found: C, 61.60; H, 3.85; N, 9.00%.

*2.3.2. Preparation of [$Mo^{VI}O_2$(fhmc-bhz)(MeOH)] (**1**)*

A solution of [$Mo^{VI}O_2(acac)_2$] (0.66 g, 2 mmol) dissolved in 5 ml of methanol was added to a stirred solution of H_2fhmc-bhz (0.64 g, 2 mmol) in methanol (10 ml) and the obtained reaction mixture was stirred at room temperature whereupon an yellow solid started to form. After 3 h of stirring, the separated solid was filtered, washed with cold methanol followed by petroleum ether and dried in a vacuum desiccator over silica gel. Yield: 0.910 g (94.7%). *Anal*. Calc. for $C_{19}H_{16}N_2O_7Mo$ (480.30): C, 47.51; H, 3.36; N, 5.83%. Found: C, 47.45; H, 3.28; N, 5.89%. X-ray diffraction quality crystals for [$Mo^{VI}O_2$(Hfhmc-bhz)(DMSO)] (**1a**) were grown by slow evaporation of a solution of **1** in DMSO.

*2.3.3. Preparations of [$Mo^{VI}O_2$(fhmc-inh)(MeOH)] (**2**), [$Mo^{VI}O_2$(fhmc-nah)(MeOH)] (**3**) and [$Mo^{VI}O_2$(fhmc-fah)(MeOH)] (**4**)*

These complexes were prepared similarly by the reaction of 2 mmol of [$Mo^{VI}O_2(acac)_2$] and 2 mmol of ligand, H_2fhmc-inh (**II**) H_2fhmc-nah (**III**) or H_2fhmc-fah (**IV**).

[$Mo^{VI}O_2$(fhmc-inh)(MeOH)] (**2**): Yield: 0.920 g (95.6%). *Anal*. Calc.for $C_{18}H_{15}N_3O_7Mo$ (481.29): C, 44.92; H, 3.14; N, 8.73 %. Found: C, 44.85; H, 3.18; N, 8.80 %.

[$Mo^{VI}O_2$(fhmc-nah)(MeOH)] (**3**): Yield: 0.936 g (97.3%). *Anal*. Calc.for $C_{18}H_{15}N_3O_7Mo$ (481.29): C, 44.92; H, 3.14; N, 8.73 %. Found: C, 44.90; H, 3.10; N, 8.78 %.

[$Mo^{VI}O_2$(fhmc-fah)(MeOH)] (**4**): Yield: 0.900 g (95.7%) *Anal*. Calc.for $C_{17}H_{14}N_2O_8Mo$ (470.26): C, 43.42; H, 3.00; N, 5.96%. Found: C, 43.48; H, 2.96; N, 5.89%.

2.4 X-Ray crystal structure determination

Three-dimensional X-ray data were collected on a Bruker Kappa Apex CCD diffractometer at room temperature for **1** by the ϕ-ω scan method. Reflections were measured from a hemisphere of data collected from frames, each of them covering 0.3° in ω. 14540 reflections measured were corrected for Lorentz and polarization effects and for absorption by multi-scan methods based on symmetry-equivalent and repeated reflections. Of them, 3113 independent reflections exceeded the significance level ($|F|/\sigma|F|$) > 4.0. After data collection, in each case an empirical absorption correction (SADABS) [26] was applied, and the structure was solved by direct methods and refined by full matrix least-squares on F^2 data using SHELX suite of programs [27]. Hydrogen atoms were included in calculation position and refined in the riding mode, except for C(2), C(9), C(10), C(11) and C(14), which were located in difference Fourier map and left to refine freely. Refinements were done with allowance for thermal anisotropy of all non-hydrogen atoms. A final difference Fourier map showed no residual density in the crystal: 0.496 and -0.727 e.Å^{-3}. A weighting scheme w = 1/[$\sigma^2(F_o^2)$ + (0.066000 P)^2 + 0.015900 P], was used in the latter stages of refinement. Further details of the crystal structure determination are given in Table 1.

<<Table 1>>

2.5. Catalytic Oxidative bromination of thymol

Thymol (1.50 g, 10 mmol), 30 % aqueous H_2O_2 (3.39g, 30 mmol), 70% $HClO_4$ (5.72 g, 40 mmol) and KBr (3.57 g, 30 mmol) were taken in water (20 mL) at room temperature. After adding catalyst (0.002 g) to the above reaction mixture, it was stirred and the obtained oxidized products were analyzed quantitatively by gas chromatography. The obtained main products were confirmed by ^{1}H NMR spectroscopy as well as GC–MS after their separations and their quantifications were made on the basis of the relative peak area of the respective product.

3. Results and discussion

3.1. Synthesis and characterization of complexes

The reaction between equimolar amounts of [$Mo^{VI}O_2(acac)_2$] and H_2fhmc-bhz (**I**), H_2fhmc-inh (**II**), H_2fhmc-nah (**III**) or H_2fhmc-fah (**IV**) in methanol results in the formation of *cis*-[$Mo^{VI}O_2$]$^{2+}$ complexes, [$Mo^{VI}O_2$(fhmc-bhz)(MeOH)] (**1**), [$Mo^{VI}O_2$(fhmc-inh)(MeOH)] (**2**)

[$Mo^{VI}O_2$(fhmc-nah)(MeOH)] (**3**) and [$Mo^{VI}O_2$(fhmc-fah)(MeOH)] (**4**), respectively. The sixth coordination site is occupied by methanol in these complexes. [Eq. (1) taking **I** as a representative example].

$$[Mo^{VI}O_2(acac)_2] + H_2fhmc\text{-}bhz + MeOH \rightarrow [Mo^{VI}O_2(fhmc\text{-}bhz)(MeOH)] + 2Hacac \quad (1)$$

Idealized structures of the complexes are shown in Scheme 2 which are based on the spectroscopic (IR, UV/Vis, ^1H and ^{13}C NMR) data, elemental analyses and X-ray diffraction study of [$Mo^{VI}O_2$(fhmc-bhz)(DMSO)] (**1a**). All these complexes are soluble in DMF and DMSO and partially soluble in methanol and acetonitrile.

<<Scheme 2>>

3.2. Thermal studies

Thermal stability of monomeric complexes **1**, **2**, **3** and **4** has been studied under an oxygen atmosphere. These complexes lose weight roughly equal to one methanol molecule in the temperature range 100-170 °C, indicating the presence of a coordinated methanol. On further increasing the temperature the solvent free complexes decompose exothermically in two/ three overlapping steps and form MoO_3 as final product. The observed MoO_3 contents of 29.2 % at ca. 615 °C for **1**, 29.0 % at 440 °C for **2**, 28.9 % at 440 °C for **3** and 29.7 % at 490 °C for **4** match closely with the calculated values of 30.0, 29.9, 29.9 and 30.6 %, respectively.

3.3. Structure descriptions

ORTEP diagram for the complex [$Mo^{VI}O_2$(Hfhmc-bhz)(DMSO)] (**1**) is shown in Fig. 1. Selected bond distances and angles are given in Table 2. In compound **1**, one complex is present in the asymmetric unit. The $O_{hydroxy}$ of methyl coumarin group, N_{azo} and $O_{benzoylhydrazide}$ atoms of the ligand, which acts as ONO tridentate, and two oxido groups coordinate to molybdenum centre. The equatorial plane is formed for these three atoms of the ligand and one of the terminal oxygen atoms. The molybdenum atom is displaced toward the apical oxido ligand from the equatorial plane by 0.3003 Å, with respect to the plane O3-O4-O5-N1 (mean deviation from plane 0.0402(15) Å) One DMSO molecule completes the coordination sphere of a distorted octahedral geometry. The O=Mo=O angle is 105.90(16)º and Mo=O distances are 1.696(3) Å and 1.695(3) Å. The Mo–O–S angle and Mo–O distance for Mo–DMSO are 126.37(18)°

(average of two angles of disordered sulphur atoms) and 2.286(3) Å, respectively, similar to other examples in literature [28,29].

The presence of intermolecular forces between the rings of methyl coumarin group and phenyl ring of benzoylhydrazide group determine the crystal packing. The π-π stacking interactions between the rings establish the linked between frameworks and determine the structure in layers (see Fig. 2). The distances between π cloud around carbon atom, C6, and the centroids of phenyl rings are: $d_{C6\text{-}c1}$ = 3.510 Å [(C6A), c1 (C13B-C14B-C15B-C16B-C17B-C18B) and repeated for other carbon-centroids].

<<Table 2>> <<Figures 1 and 2>>

3.4. IR spectral studies

Table 3 reveals a partial list of the IR spectral data. The IR spectra of the ligands H_2fhmc-bhz (**I**), H_2fhmc-inh (**II**), H_2fhmc-nah (**III**) and H_2fhmc-fah (**IV**) show four characteristic bands at 3053-3060, 1705-1716, 1673-1678, and 1586-1588 cm^{-1} due to υ(NH), $\upsilon(C{=}O)_{pyrone/hydrazide}$ and υ(C=N) stretches, respectively [30], which show their ketonic behavior in the solid state. Appearance of a new band at 1179–1200 cm^{-1} due to the ν(C-O) stretch and the absence of a υ(NH) band in all the complexes suggests the enolization of the ketonic group and replacement of H by the metal ion. A band at ca. 1703-1717 cm^{-1} due to the ketonic group of the pyrone moiety is still present in all the complexes. A very sharp band appearing at 1543-1551 cm^{-1} in complexes confirms the coordination of the azomethine nitrogen atom. This lower wavenumber band occurs due to the donation of electron density from the nitrogen atom to an empty d-orbital of the metal ion. A band appearing at 1066–1074 cm^{-1} due to υ(N–N) in ligands is also affected by the coordination of the nitrogen atom and shifts to a higher wavenumber in complexes. The presence of several medium intensity bands between 2500 and 2800 cm^{-1} in the ligands as well as in complexes suggest the existence of C–H stretching bands due to -CH_2. The $[MoO_2]^{2+}$complexes are well characterized by two prominent peaks at 936-945 and 906-920 cm^{-1}, which are assigned to $\upsilon_{asym}(O{=}Mo{=}O)$ and $\upsilon_{sym}(O{=}Mo{=}O)$ modes, respectively due to the *cis*-[MoO_2] structure [31].

<<Table 3>>

3.5. UV-Vis spectral studies

Table 4 presents absorption maxima of ligands and complexes with their extinction coefficients. The UV-Vis spectra of ligands and $[Mo^{VI}O_2]^{2+}$ complexes were recorded in DMSO. All ligands exhibit three very similar spectral bands at 380-388, 314-317 and 267-272 nm. Based on their extinction coefficient values, these bands explicate as n→π* (first two bands) and π→π* transitions, respectively. All these bands are also present in complexes with slight variations. In addition, all complexes exhibit a medium intensity band at 425 – 431 nm due to the ligand to metal charge transfer (LMCT) transition from the phenolate oxygen atom to an empty d-orbital of the molybdenum. As $[Mo^{VI}O_2]^{2+}$ complexes have $4d^0$ configuration, d→d band is not expected.

<<Table 4>>

3.6. ^{1}H and ^{13}C NMR studies

The ^{1}H NMR spectral data of ligands and complexes are collected in Table 5**.** The spectral data confirm their coordinating modes. The ^{1}H NMR spectra of a representative ligand H_2fhmc-nah (**III**) and its complex is shown in Fig. 3. The ligands show two broad signals at δ = 12.61-12.74 ppm and 12.41 – 12.57 ppm owing to the phenolic –OH and –NH, respectively. These signals disappear in the spectra of complexes due to coordination of the phenolate oxygen and enolate oxygen after replacing H by the metal ion. A signal due to azomethine proton (equivalent to 1 H) in ligands illustrates a notable downfield shifts in complexes with a coordination-induced shifts [$\Delta\delta$= [δ(complex) – δ(free ligand)] of 0.06 –0.14 ppm, confirming the coordination of the azomethine nitrogen atom. The aromatic and aliphatic protons appear in the expected regions in spectra of ligands as well as of complexes, with slight shifts in their positions.

<<Table 5>> <<Figure 3>>

Table 6 provides ^{13}C NMR spectral data of ligands and their corresponding dioxidomolybdenum (VI) complexes whereas Fig. 4 presents spectra of a representative ligand H_2fhmc-nah (**III**) and its complex (**3**). The peaks are assigned again on the basis of the coordination-induced shifts ($\Delta\delta$) of the signals for carbon atoms in the vicinity of the coordinating atoms [32].These assignments also provide useful information for the elucidation of the structures of the complexes. Ligands **I**, **II, III** and **IV** display 16, 15, 17 and 16 signals corresponding to the 18, 17, 17 and 16 carbon atoms, respectively. A total of 17, 16, 18 and 17

signals were observed for complexes **1**, **2**, **3** and **4**, respectively after coordination of ligands to the molybdenum. A large coordination induced shift of the signals for the carbon atoms associated with the phenolic oxygen (C1), the azomethine nitrogen (C11) and the enolic oxygen (C12) confirms the coordination of these functionalities to the molybdenum ion. In addition, these complexes show one signal each for coordinated MeOH at ca. 48.80 – 49.10 ppm.

<<Table 6>> <<Figure 4>>

3.7. Catalytic activity studies

Scheme 3 presents the oxidative bromination of thymol, using **1**, **2**, **3** and **4** as catalyst precursors in the presence of KBr, 70% aqueous $HClO_4$ and 30 % aqueous H_2O_2 under an aqueous system. The bromination reaction takes place on the most activated site as a result of electrophilic aromatic substitution in the phenolic ring. Particularly, the bromination reaction led to the formation of two isomers, 4-bromothymol and 2-bromothymol; 4-bromothymol being the major product due to steric hindrance at the *ortho* position. Further bromination of the *para* isomer gave 2,4- dibromothymol in excellent yield.

Consequently, the reaction has been investigated by changing different parameters that may affect the rate of thymol bromination and the selectivity of products.

<<Scheme 3>>

Reaction conditions were optimized for considering different parameters like amounts of catalyst, 30% aqueous H_2O_2, KBr and $HClO_4$ using $[Mo^{VI}O_2(fhmc\text{-}bhz)(MeOH)]$ (**1**) as a representative catalyst precursor. Thus, for 10 mmol of thymol (1.50 g), three different amounts of catalyst (0.001, 0.002 and 0.003 g), 30 % aqueous H_2O_2 (10, 20 and 30 mmol), KBr (10, 20 and 30 mmol) and 70% $HClO_4$ (10, 20, 30 and 40 mmol, added in four equal portions to the reaction mixture, first portion at t = 0 and other three portions after every 30 min intervals) were taken in 20 mL water and the reaction was carried out at room temperature. The $HClO_4$ was found to be crucial to bring out catalytic bromination and its amount has great influence on the conversion and selectivity of products. The complexes slowly decompose during the reaction; decomposition is slowed down, if $HClO_4$ is successively added in four equal portions during 2 h of reaction time.

Table 7 presents all the conditions considered and the corresponding percentage of oxidative bromination of thymol along with the selectivity of different reaction products. It is clear from the data shown in table that the conversions and the selectivity of products differ on varying the reagents. However, the best appropriate reaction conditions (entry no. 10 of Table 7) for the maximum oxidative bromination of thymol with 94% conversion are: catalyst (0.002 g), H_2O_2 (3.39 g, 30 mmol), KBr (3.57 g, 30 mmol) and $HClO_4$ (5.72 g, 40 mmol) in 20 mL water. Under these conditions the selectivity of different major products follows the order: 2,4-dibromothymol (84.6%) > 2-bromothymol (8.4%) > 4-bromothymol (7%). Using 0.002 g of catalyst and considering the substrate to different reagents in the molar ratio presented in entry no 15 of Table 7 gave highest selectivity (85.3%) of 4-bromothymol amongst all the conditions applied. Increasing the amounts of KBr or acid results in the formation of more 2,4-dibromo thymol product at the expense of 4-bromo product. Under the optimized conditions for the maximum conversion of thymol, other catalysts i.e. **2**, **3** and **4** exhibit similar catalytic activity along with similar selectivity of different products (entry no 11, 12 and 13). Blank reaction i.e without catalyst, under same conditions (entry no. 16 of Table 7) resulted in 54% conversion. Thus, these complexes enhance conversion of thymol and alter the products yield.

<<Table 7>>

The oxidative bromination of thymol and the selectivity of different reaction products for catalyst **1** under the optimized reaction conditions (see Table 8) have also been studied in different solvents. Though, conversion of thymol is almost same in all solvents, the selectivity of products varies. In H_2O, H_2O/CH_2Cl_2 and $H_2O/CHCl_3$, all three products were obtained and the selectivity followed the order: 2,4-dibromothymol > 2-bromothymol> 4-bromothymol, whereas H_2O/MeOH and H_2O/MeCN systems gave only two products; 2,4–dibromothymol being a major one and 2-bromothymol a minor. With all three products in H_2O/hexane, the selectivity follows the order: 2,4–dibromothymol (77.7%) > 4-bromothymol (17.6%) >2-bromothymol (4.7%).

<<Table 8>>

3.8. Reactivity of dioxidomolybdenum(VI) complexes and possible mechanism for catalytic oxidation of substrate.

As reported earlier, dioxidomolybdenum(VI) complexes react with H_2O_2 to give the corresponding $[Mo^{VI}O(O_2)]^{2+}$ complexes [33]. Such species has been generated in DMSO and

monitored by UV-vis spectroscopy. In a typical reaction, 20 mL of 4.0×10^{-5} M solution of [$Mo^{VI}O_2$(fhmc-bhz)(MeOH)] was treated with a drop wise solution prepared by dissolving 30% aqueous H_2O_2 (0.904 g, 8.0 mmol) in 5 mL of DMSO and the observed spectroscopic changes are depicted in Fig. 5 (a). The intensity of the bands at 322 and 261 nm considerably increases and finally disappears. The broad charge transfer band appearing at 425 nm slowly decreases in intensity [Fig. 5(a)] along with broadening and finally vanishes. Simultaneously, a band at ca. 378 nm also decreases in intensity and disappears. These changes in spectra occur due to the interaction of H_2O_2 with the complex and plausible formation of [$Mo^{VI}O(O_2)$(fhmc-bhz)] in DMSO. Similar spectral changes have also been noted for other complexes; Figs. 5(b–d).

In the model vanadium complex system studied in bi-phasic system for oxidative bromination, initially the intermediate oxidoperixidovanadium(V) derivative forms in the presence of H_2O_2 which oxidizes Br^- to HOBr/Br_2. This intermediate enters into organic phase where the bromination of appropriate organic substrates takes place [22,34]. During this process acid probably promotes the protonation of the peroxide intermediate. A similar mechanism may also be proposed here.

<<Figure 5>>

4. Conclusions

The dioxidomolybdenum(VI) complexes [$Mo^{VI}O_2$(fhmc-bhz)(MeOH)] (**1**), [$Mo^{VI}O_2$(fhmc-inh)(MeOH)] (**2**) [$Mo^{VI}O_2$(fhmc-nah)(MeOH)] (**3**) and [$Mo^{VI}O_2$(fhmc-fah)(MeOH)] (**4**) have been prepared from potential dibasic tridentate ONO type ligands H_2fhmc-bhz (**I**), H_2fhmc-inh (**II**), H_2fhmc-nah (**III**) and H_2fhmc-fah (**IV**), respectively and cgharacterized. These complexes are good catalyst precursors for the oxidative bromination of thymol in the presence of green oxidant 30 % H_2O_2, $HClO_4$ and bromide ion, therefore acting as functional models of vanadium dependent haloperoxidases. $[Mo^{VI}O_2]^{2+}$ complexes upon treatment with H_2O_2 instantly generates $[Mo^{VI}O(O_2)]^{2+}$ species which ultimately oxidizes Br^- to HOBr/ Br_2 in the presence of acid. This species brominates the thymol and give corresponding brominating products in high yield of ca. 94-99% under optimized reaction conditions. The conversion of thymol is generally same in different solvents but the number of products and their selectivity are solvent dependent.

Acknowledgments

S.D. acknowledges the University Grant Commission, New Delhi, India for a Senior Research fellowship.

Appendix A. Supplementary data

CCDC 1056678 contains the supplementary crystallographic data for the structure reported in this paper. These data can be obtained free of charge via http://www.ccdc.cam.ac.uk/conts/retrieving.html, or from the Cambridge Crystallographic Data Centre, 12 Union Road, Cambridge CB2 1EZ, UK; fax: (+44) 1223 336 033; or e-mail: deposit@ccdc.cam.ac.uk. Supplementary data associated with this article can be found, in the online version, at doi: $$$$$.

References

[1] P. K. Ajikumar, K. Tyo, S. Carlsen, O. Mucha, T. H. Phon G. Stephanopoulos, Mol. Pharmaceutics 5 (2008) 167.

[2] Carla C.C.R. de Carvalho, M. Manuela R. da Fonseca, Biotechnol. Adv. 24 (2006) 134.

[3] M. S. Yusubo, L. A. Drygunov, A. V. Tkachev, V. V. Zhdankin, Arkivoc IV (2005) 179.

[4] S.A. Kotharkar, S.S. Bahekar, D.B. Shinde, Mendeleev Commun. 16 (2006) 241.

[5] G. Kokotos, V. Theodorou, C. Tzougraki, Bioorg. Med. Chem. Lett. 7 (1997) 2165.

[6] A. Karaliota, O. Kretsi, C. Tzougraki, J. Inorg. Biochem. 84 (2001) 33.

[7] I. Kostova, I. Manolov, I. Nicolova, S. Konstantinov, M. Karaivanova, Eur. J. Med. Chem. 36 (2001) 339.

[8] A.B. Dongmo, A.G.B. Azebaze, T.B. Nguelefack, B.M. Ouahouo, B. Sontia, M. Meyer, A.E. Nkengfack, A. Kamanyi, W. Vierling, J. Ethnopharmacol. 111 (2007) 329.

[9] Z.S. Tong, M.X. Huang, C.S. Dai, Chinese J. Med. Chem. 4 (1994) 150.

[10] S. Pasayat, S. P. Dash, Saswati, P. K. Majhi, Y. P. Patil, M. Nethaji, H. R. Dash, S. Das, R. Dinda, Polyhedron 38 (2012)198.

[11] M.R. Maurya, S. Dhaka, F. Avecilla, New J. Chem. 39 (2015) 2130.

[12] S. Pasayat, S.P. Dash, S. Roy, R. Dinda, S. Dhaka, M.R. Maurya, W. Kaminsky, Y.P. Patiland, M. Nethaji, Polyhedron 67 (2014) 1.

[13] A.C. Cunha, J.M. Figueiredo, J.L.M. Tributino, A.L.P. Miranda, H.C. Castro, R.B. Zingali, C.A.M. Fraga, M.C.B.V. Souza, V.F. Ferreira, E.J. Barreiro, Bioorg. Med. Chem. 11 (2003) 2051.

[14] M.R. Maurya, S. Dhaka, F. Avecilla, Polyhedron 67 (2014) 145.

[15] J.J. Boruah, S.P. Das, R. Borah, S.R. Gogoi, N.S. Islam, Polyhedron 52 (2013) 246.

[16] R.D. Chakravarthy, D.K. Chand, J. Chem. Sci. 123 (2011) 187.

[17] S. S. Salih, Br. J. Pharmacol. Toxicol. 3 (2012) 147.

[18] (a) G.W. Gribble, Chem. Soc. Rev. 28 (1999) 335; (b) M. Liu, P.E. Hansen, X. Lin, Mar. Drugs 9 (2011) 1273; (c) B.G. Wang, J.B. Gloer, N.Y. Ji, J.C. Zhao, Chem. Rev. 113 (2013) 3632.

[19] D. Wischang, O. Brücher, J. Hartung, Coord. Chem. Rev. 255 (2011) 2204.

[20] R. Kaur, M. P. Darokar, S. K. Chattopadhyay, V. Krishna, A. Ahmad, Med. Chem. Res. 23 (2014) 2212.

[21] L. Getrey, T. Krieg, F. Hollmann, J. Schrader, D. Holtmann, Green Chem. 16 (2014) 1104.

[22] F. Sabuzi, E. Churakova, P. Galloni, R. Wever, F. Hollmann, B. Floris, V. Conte, Eur. J. Inorg. Chem. (2015), DOI:10.1002/ejic.201500086.

[23] G.J.J. Chen, J. W. McDonald, W. E. Newton, Inorg. Chem. 15 (1976) 2612.

[24] K. S. S. Lamani, O. Kotresh, M. A. Phaniband, J.C. Kadakol, E-J. Chem. 6 (2009) S239.

[25] M.R. Maurya, M. Bisht, F. Avecilla, Indian J. Chem. 50A (2011) 1562.

[26] G. M. Sheldrick, *SADABS*, version 2.10, University of Göttingen, Germany (2004).

[27] *SHELX*, G. M. Sheldrick, Acta Crystallogr., Sect. A 64 (2008) 112.

[28] N.K. Ngan, K.M. Lo, C.S.R. Wong, Polyhedron 30 (2011) 2922.

[29] M.R. Maurya, L. Rana, F. Avecilla, Inorg. Chim. Acta 429 (2015) 138.

[30] M.R. Maurya, S. Khurana, Shailendra, A. Azam, W. Zhang, D. Rehder, Eur. J. Inorg. Chem. 10 (2003) 1966.

[31] A. Syamal and M.R. Maurya, Coord. Chem. Rev. 95 (1989) 183.

[32] A.D. Keramidas, A.B. Papaioannou, A. Vlahos, T.A. Kabanos, G. Bonas, A. Makriyannis, C.P. Rapropoulou, A. Terzis, Inorg. Chem.35 (1996) 357.

[33] M.R. Maurya, N. Kumar, F. Avecilla, J. Mol. Catal. A: Chem. 392 (2014) 50.

[34] V. Conte, B. Floris, Inorg. Chim. Acta 363 (2010) 1935.

Schemes

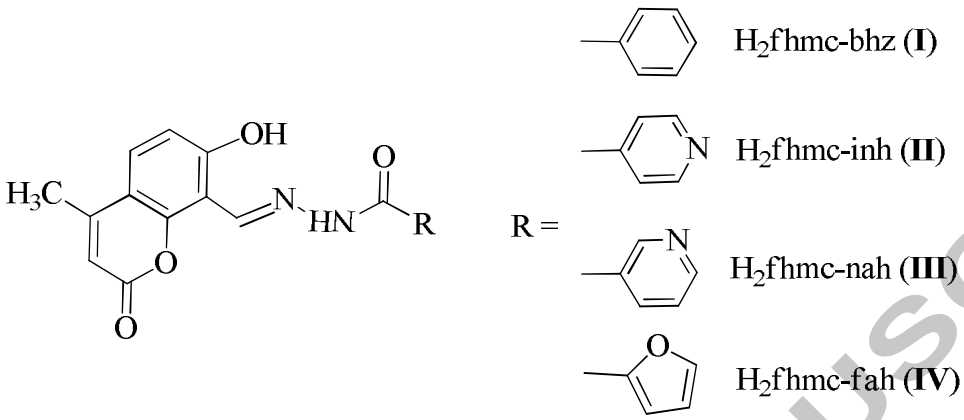

Scheme 1. Structure of the ligands designated by **I**, **II, III** and **IV** used in this work.

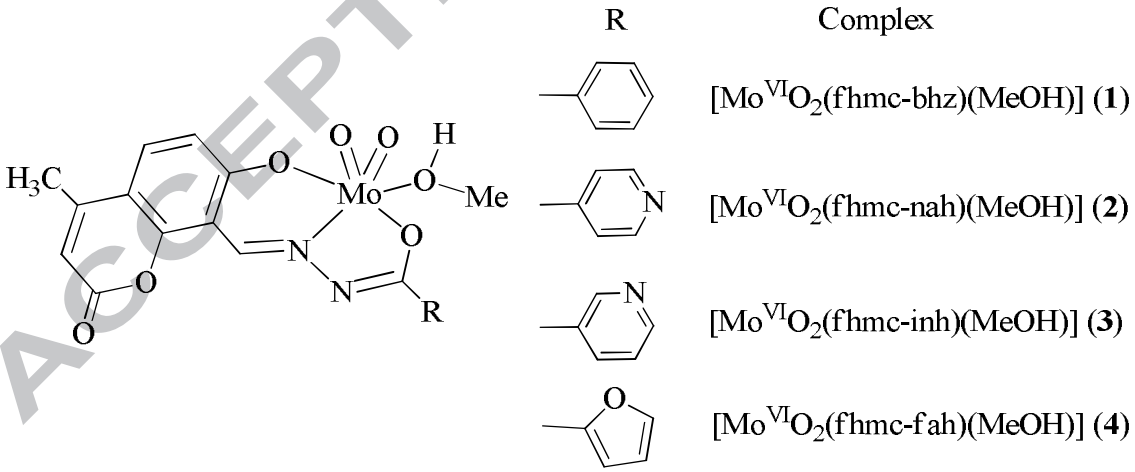

Scheme 2. Proposed structure of *cis*-$[Mo^{VI}O_2]^{2+}$complexes.

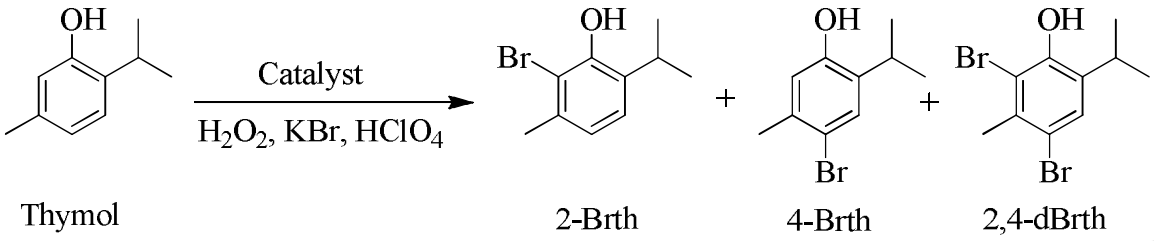

Scheme 3. Products of the oxidative bromination of thymol. 2-Brth = 2-bromothymol, 4-Brth = 4-bromothymol, 2,4-dBrth = 2,4-dibromothymol.

Tables

Table 1

Crystal Data and Structure Refinement for the complexes [$Mo^{VI}O_2$(Hfhmc-bhz)(DMSO)] (**1**).

	1
Formula	C_{20} H_{18} Mo N_2 O_7 S
Formula weight	526.36
T, *K*	293
Wavelength, Å	0.71073
Crystal system	Triclinic
Space group	P $\bar{1}$
a/Å	8.7732(3)
b/Å	8.9318(3)
c/Å	13.2399(5)
α/°	86.631(2)
β/°	88.075(2)
γ/°	86.938(2)
V/Å^3	1033.73(6)
Z	2
F_{000}	532
D_{calc}/g cm^{-3}	1.691
μ/mm^{-1}	0.782
θ/ (°)	1.54 to 25.57
R_{int}	0.0401
Crystal size/ mm^3	0.22 x 0.21 x 0.18
Goodness-of-fit on F^2	1.105
$R_1[I>2\sigma(I)]$ [a]	0.0386
wR_2 (all data) [b]	0.1138
Largest differences peak and hole (eÅ^{-3})	0.496 and -0.727

[a] $R_1 = \Sigma \left| \left| F_o \right| - \left| F_c \right| \right| / \Sigma \left| F_o \right|$. [b] $wR_2 = \{\Sigma[w(\left| \left| F_o \right|^2 - \left| F_c \right|^2 \right|)^2] / \Sigma[w(F_o^2)^2]\}^{1/2}$

Table 2

Bond lengths [Å] and angles [°] for [$Mo^{VI}O_2$(Hfhmc-bhz)(DMSO)] (**1**).

Bond lengths	**1**
Mo(1)-O(3)	1.937(3)
Mo(1)-O(4)	1.999(3)
Mo(1)-O(5)	1.696(3)
Mo(1)-O(6)	1.695(3)
Mo(1)-O(1S)	2.286(3)
Mo(1)-N(1)	2.243(3)
N(1)-C(11)	1.294(5)
N(1)-N(2)	1.396(4)
N(2)-C(12)	1.313(5)

Angles	**1**
O(6)-Mo(1)-O(5)	105.90(16)
O(6)-Mo(1)-O(3)	97.81(13)
O(5)-Mo(1)-O(3)	103.21(13)
O(6)-Mo(1)-O(4)	95.43(13)
O(5)-Mo(1)-O(4)	97.65(13)
O(3)-Mo(1)-O(4)	151.10(12)
O(6)-Mo(1)-N(1)	94.25(14)
O(5)-Mo(1)-N(1)	158.32(13)
O(3)-Mo(1)-N(1)	81.39(11)
O(4)-Mo(1)-N(1)	72.08(11)
O(6)-Mo(1)-O(1S)	167.83(13)
O(5)-Mo(1)-O(1S)	86.06(13)
O(3)-Mo(1)-O(1S)	81.23(11)
O(4)-Mo(1)-O(1S)	80.47(10)
N(1)-Mo(1)-O(1S)	73.60(11)
S(1A)-O(1S)-Mo(1)	125.34(17)

S(1B)-O(1S)-Mo(1)	127.4(2)

Table 3

IR spectral data [in cm^{-1}] of compounds.

Compounds	ν(NH)	$\nu(C=O)_{pyrone/hydrazide}$	ν(C=N)	ν(C-O)	ν(O=Mo=O)[a]
H_2fhmc-bhz (**I**)	3060	1705, 1673	1586		
H_2fhmc-inh(**II**)	3058	1710, 1678	1588		
H_2fhmc-nah (**III**)	3056	1713, 1676	1586		
H_2fhmc-fah (**IV**)	3053	1716, 1674	1587		
$[Mo^{VI}O_2$(fhmc-bhz)(MeOH)] (**1**)		1703, 1624	1551	1182	938, 906
$[Mo^{VI}O_2$(fhmc-inh)(MeOH)] (**2**)		1707, 1621	1547	1179	945, 915
$[Mo^{VI}O_2$(fhmc-nah)(MeOH)] (**3**)		1711, 1616	1551	1200	936, 906
$[Mo^{VI}O_2$(fhmc-fah)(MeOH)] (**4**)		1717, 1611	1543	1180	938, 920

[a]Asymmetric and symmetric ν(O=Mo=O) values.

Table 4

UV-vis spectral data of ligands and complexes recorded in methanol.

Compound	λ_{max} /nm (ε/ M^{-1} cm^{-1})
H_2fhmc-bhz (**I**)	272 (1.8×10^4), 317 (3.1×10^4), 380 (7.6×10^3)
H_2fhmc-inh(**II**)	268 (8.8×10^3), 317 (2.3×10^4), 382 (3.2×10^3)
H_2fhmc-nah (**III**)	267 (7.8×10^3), 314 (2.4×10^4), 381 (2.1×10^3)
H_2fhmc-fah (**IV**)	270 (9.5×10^3), 317 (2.6×10^4), 388 (5.7×10^3)
$[Mo^{VI}O_2$(fhmc-bhz)(MeOH)] (**1**)	261 (1.8×10^4), 322 (2.8×10^4), 378 (1.0×10^4), 425 (4.3×10^3)
$[Mo^{VI}O_2$(fhmc-inh)(MeOH)] (**2**)	259 (1.2×10^4), 318 (2.3×10^4), 382 (6.1×10^3), 430 (2.4×10^3)
$[Mo^{VI}O_2$(fhmc-nah)(MeOH)] (**3**)	261 (1.3×10^4), 318 (2.9×10^4), 380 (6.0×10^3), 431 (2.7×10^3)
$[Mo^{VI}O_2$(fhmc-fah)(MeOH)] (**4**)	267 (1.4×10^4), 317 (3.3×10^4), 379 (7.2×10^3), 430 (3.0×10^3)

Table 5

^{1}H NMR chemical shifts [a] [δ in ppm] of ligands and complexes recorded in DMSO-d_6.

Compounds	-CH=N-	Aromatic H	-OH	–NH	-CH_3
I	9.06	6.18 (d, 1H), 6.88 (t, 1H), 7.54 (t, 2H), 7.61 (t, 2H), 7.94 (t, 2H)	12.74	12.41	2.35
1	9.14	6.34 (s, 1H), 6.97 (d, 1H), 7.51 (t, 2H), 7.59	-	-	2.42
$\Delta\delta$	(0.08)	(t, 1H), 7.89 (d, 1H), 8.03 (d, 2H)			
II	9.07	6.22 (s, 1H), 6.91 (d, 1H), 7.66 (d, 1H), 7.85 (d, 2H), 8.81 (s, 2H)	12.63	12.57	2.36
2	9.21	6.34 (s, 1H), 6.99 (d, 1H), 7.93 (s, 3H), 8.77	-	-	2.43
$\Delta\delta$	(0.14)	(s, 2H)			
III	9.11	6.22 (s, 1H), 6.92 (d, 1H), 7.66 (s, 1H), 7.68 (d, 1H), 8.28 (d, 1H), 8.79 (s, 1H), 9.07 (s, 1H)	12.61	12.55	2.37
3	9.18	6.35 (s, 1H), 6.99 (d, 1H), 7.57 (s, 1H), 7.91	-	-	2.50
$\Delta\delta$	(0.07)	(d, 1H), 8.35 (d, 2H), 8.78 (s,1H)			
IV	9.07	6.26 (s, 1H), 6.73 (s, 1H), 6.75 (d, 1H), 7.35 (s, 1H), 7.70 (d, 1H), 8.00 (s,1H)	12.66	12.51	2.40
4	9.13	6.34 (s, 1H), 6.73 (s, 1H), 6.97 (d, 1H), 7.27	-	-	2.40
$\Delta\delta$	(0.06)	(d, 1H), 7.88 (d, 1H), 7.98 (s, 1H)			

[a] Letters given in parentheses indicate the signal structure: s = singlet, d = doublet.

Table 6

^{13}C NMR spectral data [δ in ppm] of ligand and complexes.

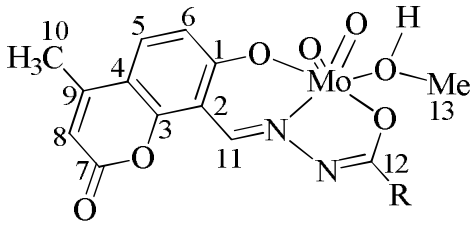

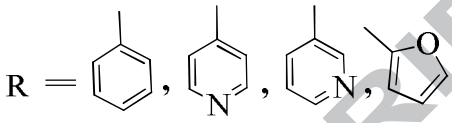

Compound	C1	C2- C9	C10	C11	C12	C13	R		
I	159.71	113.90, 152.90, 106.11,128.48, 112.25, 161.56, 111.20,154.28	18.80	143.97	162.90	-	132.83, 132.53	128.16,	129.16,
1 ($\Delta\delta$)	154.12 (–5.59)	113.89, 132.81, 106.23, 128.65, 112.00, 154.21, 108.65, 149.30	18.84	162.40 (18.43)	169.65 (6.75)	48.80	129.95, 131.36	115.93,	129.36,
II	159.66	113.96, 151.04, 105.82, 128.91 112.33, 161.46, 111.29, 154.32	18.83	145.21	161.59	-	139.58, 121.90, 153.04		
2 ($\Delta\delta$)	152.75 (–6.91)	115.92, 136.24, 108.79, 127.12, 113.28, 154.90, 112.43, 149.56	19.30	162.13 (16.92)	168.19 (6.60)	48.90	128.50, 122.76, 132.43		
III	159.64	113.94, 153.24, 105.88, 128.41, 112.34, 161.54, 111.23, 154.34	18.77	144.70	161.65		135.89, 128.81, 124.24, 149.12, 153.02		
3 ($\Delta\delta$)	154.11 (–5.53)	115.93, 149.35, 108.55, 131.60, 113.96, 159.28, 112.05, 153.06	18.81	162.40 (17.70)	168.06 (6.41)	49.05	126.20, 150.14	136.15,	124.53,
IV	154.44	114.10, 146.28, 111.24, 114.21 112.90, 159.77, 112.39, 153.00	18.91	144.20	161.50	-	128.17, 116.18	113.87,	106.09,
4 ($\Delta\delta$)	152.18 (–2.26)	117.38, 147.79, 113,27, 131.35, 115.94, 159.37, 114.01, 149.03	18.89	162.23 (18.03)	168.35 (6.85)	49.10	147.06, 144.58	108.71,	112.16,

Table 7

Conversion of thymol (1.50g, 10 mmol), TOF and product selectivity using [$Mo^{VI}O_2$(fhmc-nah)(MeOH)] (**1**) as a catalyst precursor in 2 h of reaction time under different reaction conditions.

Entry No.	KBr [g (mmol)]	H_2O_2 [g (mmol)]	$HClO_4$ [g (mmol)]	Catalyst [g (mmol)]	Conv. [%]	TOF [h^{-1}]	2-Brth	4-Brth	2,4-dBrth
1.	1.19 (10)	1.13 (10)	1.43 (10)	0.001 (2.0×10^{-3})	14	171	15.3	84.7	0
2	1.19 (10)	1.13 (10)	1.43 (10)	0.002 (4.1×10^{-3})	24	293	14.7	83.3	1
3	1.19 (10)	1.13 (10)	1.43 (10)	0.003 (6.2×10^{-3})	27	330	16.2	83.8	2
4	1.19 (10)	2.27 (20)	1.43 (10)	0.002 (4.1×10^{-3})	37	451	12.7	85	2.3
5	1.19 (10)	3.39 (30)	1.43 (10)	0.002 (4.1×10^{-3})	45	549	13.3	84.3	2.4
6	2.38 (20)	3.39 (30)	1.43 (10)	0.002 (4.1×10^{-3})	62	750	8.5	57	34.5
7	3.57 (30)	3.39 (30)	1.43 (10)	0.002 (4.1×10^{-3})	71	872	9.2	52	38.8
8	3.57 (30)	3.39 (30)	2.86 (20)	0.002 (4.1×10^{-3})	79	956	4.2	32.3	63.5
9	3.57 (30)	3.39 (30)	4.29 (30)	0.002 (4.1×10^{-3})	86	1048	4.0	18.7	77.3
10	3.57 (30)	3.39 (30)	5.72 (40)	0.002 (4.1×10^{-3})	94	1146	8.4	7	84.6
11[a]	3.57 (30)	3.39 (30)	5.72 (40)	0.002 (4.1×10^{-3})	99	1207	8.3	8	83.7
12[b]	3.57 (30)	3.39 (30)	5.72 (40)	0.002 (4.1×10^{-3})	98	1195	6.3	5.4	88.3
13[c]	3.57 (30)	3.39 (30)	5.72 (40)	0.002 (4.1×10^{-3})	97	1155	6.5	4.2	89.3
14	2.38 (20)	2.27 (20)	2.86 (20)	0.002 (4.1×10^{-3})	60	731	12.5	82.2	5.3
15	2.38 (20)	2.27 (20)	4.29 (30)	0.002 (4.1×10^{-3})	73	890	12.6	85.3	2.1
16	3.57 (30)	3.39 (30)	5.72 (40)	blank	54	-	20.7	26	53.3

[a][$Mo^{VI}O_2$(fhmc-inh)(MeOH)] (**2**)

[b][$Mo^{VI}O_2$(fhmc-nah)(MeOH)] (**3**)

[c][$Mo^{VI}O_2$(fhmc-fah)(MeOH)] (**4**)

Table 8

Solvents effect on the selectivity of product.

Solvents	Conversion [%]	2-Brth	4-Brth	2,4-dBrth
H_2O	94	8.4	7	84.6
H_2O/CH_2Cl_2	99	9.1	1.3	89.6
$H_2O/CHCl_3$	99	13.2	3.4	86.4
H_2O/MeOH	99	13.6	-	86.4
H_2O/MeCN	99	13.3	-	86.7
H_2O/Hexane	97	4.7	17.6	77.7

Figures

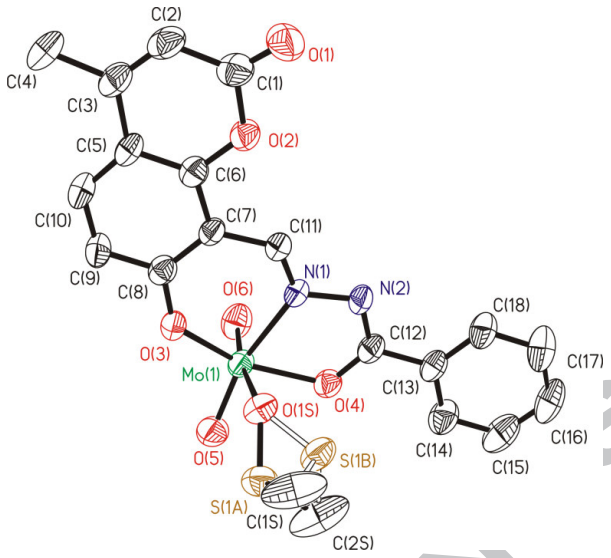

Fig. 1. ORTEP plot of [Mo^{VI}O$_2$(Hfhmc-bhz)(DMSO)] (**1**). All the non-hydrogen atoms are presented by their 50% probability ellipsoids. Hydrogen atoms are omitted for clarity.

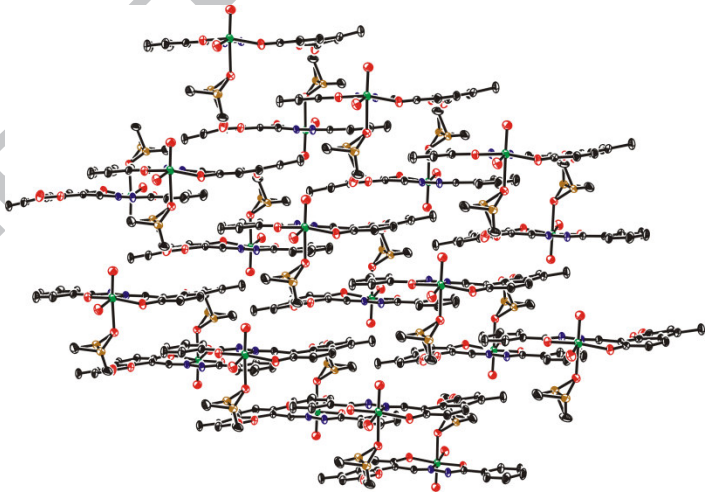

Fig. 2. Crystal packing of [Mo^{VI}O$_2$(Hfhmc-bhz)(DMSO)] (**1**). Layer structure linked by π-π-stacking interactions (see Fig. 2).

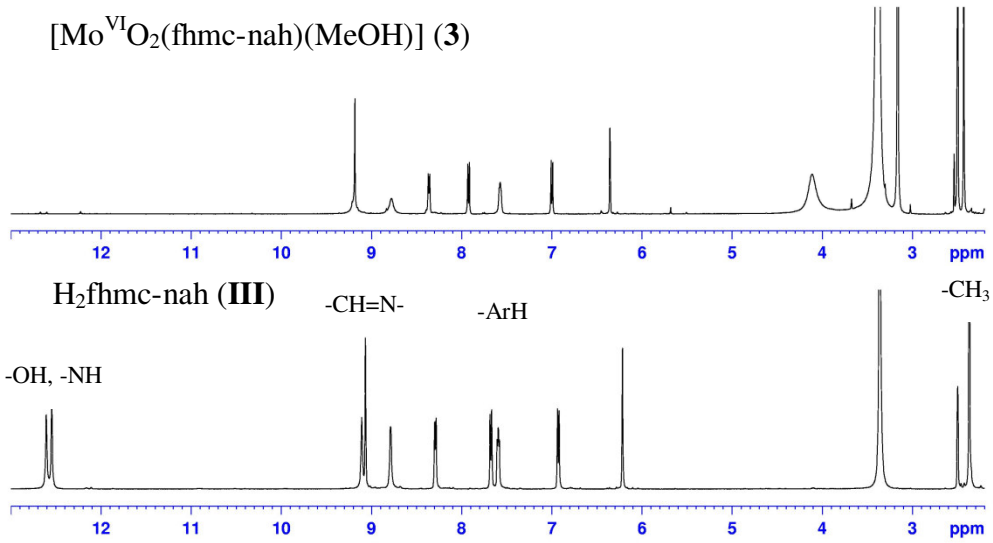

Fig. 3. ^{1}H NMR spectra of H_2fhmc-nah (**III**) and [$Mo^{VI}O_2$(fhmc-nah)(MeOH)] (**3**).

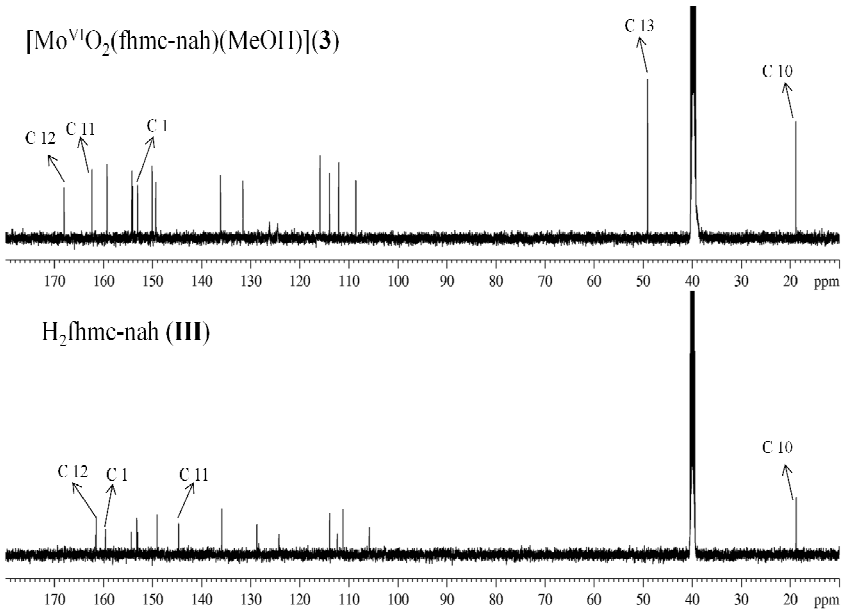

Fig. 4. ^{13}C NMR spectra of H_2fhmc-nah (**III**) and [$Mo^{VI}O_2$(fhmc-nah)(MeOH)] (**3**).

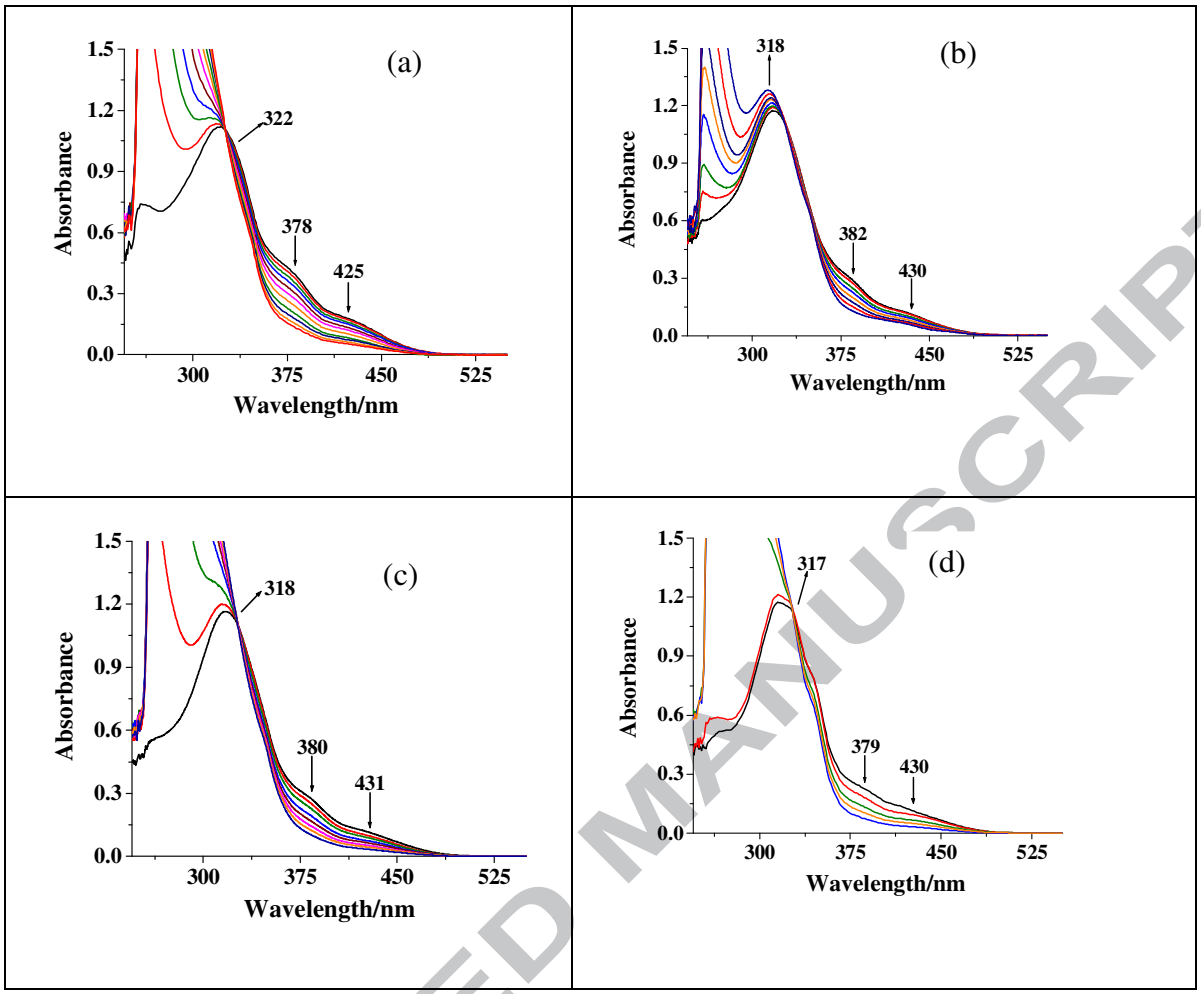

Fig. 5. Spectral changes observed during the titration of dioxidomolybdenum(VI) complexes. (a) The spectra were recorded after successive addition of one drop portion of H_2O_2 [30% H_2O_2 (0.904 g, 8.0 mmol) dissolved in 5 mL of DMSO; final concentration of H_2O_2 = 1.59 M)] to 20 mL of 4.0× 10^{-5} M solution of [$Mo^{VI}O_2$(fhmc-bhz)(MeOH)]. (b) The spectra were recorded after successive addition of one drop portion of H_2O_2 [30% H_2O_2 (0.990 g, 8.8 mmol) dissolved in 5 mL of DMSO; final concentration of H_2O_2 = 1.74 M)] to 20 mL of 5 × 10^{-5} M solution of [$Mo^{VI}O_2$(fhmc-inh)(MeOH)]. (c) The spectra were recorded after successive addition of one drop portion of H_2O_2 [30% H_2O_2 (0.825 g, 7.3 mmol) dissolved in 5 mL of DMSO; final concentration of H_2O_2 = 1.45 M] to 20 of mL of 4 × 10^{-5} M solution of [$Mo^{VI}O_2$(fhmc-nah)(MeOH)]. (d) The spectra were recorded after successive addition of one drop portion of H_2O_2 [30% H_2O_2 (0.938 g, 8.3 mmol) dissolved in 5 mL of DMSO; final concentration of H_2O_2 = 1.65 M] to 20 of mL of 3.5 × 10^{-5} M solution of [$Mo^{VI}O_2$(fhmc-fah)(MeOH)].

Graphical abstract

Oxidative bromination of monoterpene (thymol) using dioxidomolybdenum (VI) complexes of hydrazones of 8-formyl-7-hydroxy-4-methylcoumarin

Mannar R. Maurya, Sarita Dhaka, Fernando Avecilla

Oxidative bromination of thymol catalyzed by dioxidomolybdenum(VI) complexes are reported.

Oxidative bromination of monoterpene (thymol) using dioxidomolybdenum (VI) complexes of hydrazones of 8-formyl-7-hydroxy-4-methylcoumarin

Mannar R. Maurya, Sarita Dhaka, Fernando Avecilla

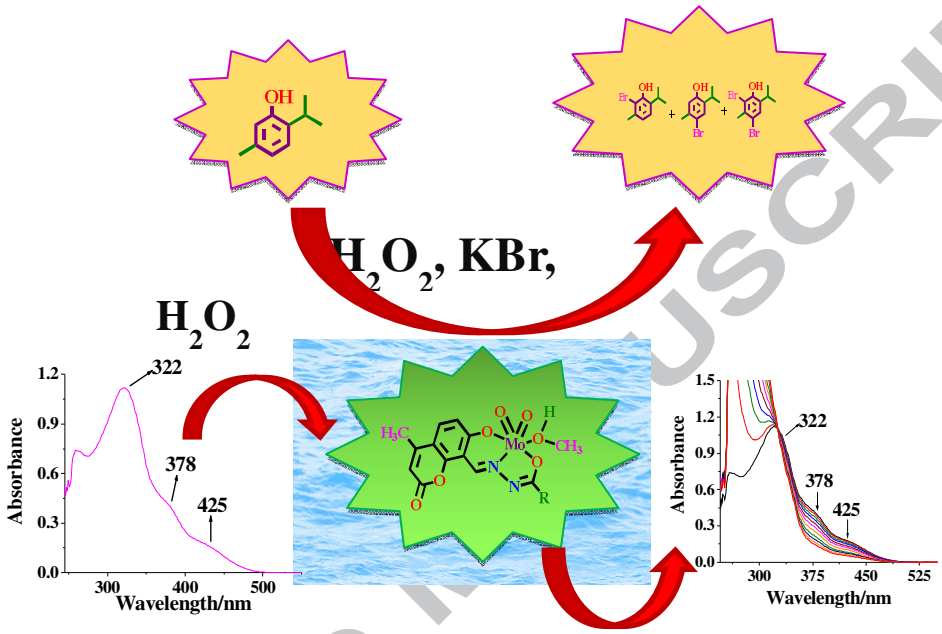

Oxidative bromination of monoterpene thymol using dioxidomolybdenum(VI) complexes of hydrazones of 8-formyl-7-hydroxy-4-methylcoumarin

Mannar R. Maurya, Sarita Dhaka, Fernando Avecilla

Research Highlights

1. New dioxidomolybdenum(VI) complexes of 8-formyl-7-hydroxy-4-methylcoumarin derived ONO donor ligands are reported.
2. Crystal structure of one of the complexes, [$Mo^{VI}O_2$(fhmc-bhz)(MeOH)] (**1**) is reported.
3. These complexes catalyze the oxidative bromination of thymol using 30 % H_2O_2 at room temperature.
4. These complexes act as functional models of vanadium dependent haloperoxidases.